ELSEVIER

PII: S0032-3861(97)10327-5

Polymer Vol. 39 No. 16, pp. 3801–3807, 1998

0032-3861/98/$19.00+0.00

The application of a new configurational entropy model to the structural relaxation in an epoxy resin

S. Montserrat[a,*], J. L. Gómez Ribelles[b] and J. M. Meseguer[c]
[a]*E.T.S. Enginyers Industrials, Universitat Politècnica de Catalunya, Carrer Colom 11, E-08222 Terrassa, Spain*
[b]*Departament de Termodinàmica Aplicada, Universitat Politècnica de València, PO Box 22012, E-46071 València, Spain*
[c]*Departament de Física Aplicada, Universitat Politècnica de València, PO Box 22012, E-46071 València, Spain*
(Received 14 June 1997; revised 13 October 1997)

The aim of this work is to model the structural relaxation of a fully cured epoxy resin. The samples were subjected to thermal treatments involving isothermal annealing at temperatures T_a for times t_a before the measuring scan carried out on heating in the DSC. The values of T_a ranged between $T_g - 8$ and $T_g - 50$°C and those of t_a between 0 and 16000 min. A new model based on the evolution of the configurational entropy was used to simulate the experimental data, obtained previously by one of the authors. A curve of calorimetric relaxation times as a function of reciprocal temperature and the β parameter of the KWW equation were determined from a comparison between experimental and calculated thermograms. Using the peak shift method, the Narayanaswamy parameter x was determined from both the experimental and simulated scans. The calorimetric relaxation times are compared with those found for dielectric and dynamic-mechanical relaxation.

(Keywords: epoxy resin; glass transition; structural relaxation)

INTRODUCTION

Structural relaxation is the process of approach to an equilibrium state undergone by a glass held in constant enviromental conditions after its formation history. The kinetics of the process can be characterized by the time dependence of different properties of the material: specific volume or enthalpy, mechanical or dielectric properties, etc. The kinetics may be quite different depending on the variable selected for the study, i.e. on the experimental technique.

Much attention has been focused on the description of the kinetics of the process by means of phenomenological models[1–5], and on establishing the physical significance of the adjustable parameters that these models contain. In this respect, differential scanning calorimetry (DSC) has been the experimental technique most widely applied.

In DSC experiments the results consist of a series of heat capacity $c_p(T)$ or heat flux $\dot{q}(T)$ curves measured in heating scans (which we will call thermograms) from a temperature T_1 below the glass transition temperature T_g to a temperature T_0 above T_g. Previously, the samples have been subjected to a thermal treatment that may or may not include an isothermal period at an annealing temperature T_a for a certain annealing time t_a.

The set of parameters of the model are determined to make the model simulation for the experiments as close as possible to the experimental data, usually by means of a least-squares routine. The essential test for the validity of phenomenological models is to check whether or not the parameters thus determined are in fact material parameters independent of the thermal history, i.e. whether the model equations with a single set of parameters can reproduce accurately the experimental thermograms measured after different thermal histories. Several works have shown that this is not easy in the case of the Scherer–Hodge or the Narayanaswamy–Moynihan models[6–9].

Recently Gómez Ribelles *et al.*[10–12] proposed a model that follows the evolution of the configurational entropy S_c during the structural relaxation process. In the present paper, the applicability of this new model is checked against a series of experimental DSC data on a fully cured epoxy resin, obtained previously by one of the authors[13,14].

The model retains the main assumptions of the model proposed by Scherer and Hodge (SH model)[3,4] (it uses the Adam–Gibbs[15] equation for the dependence of the relaxation time on T and S_c, in addition to the usual assumptions of linearization by means of the reduced time[2,16], thermorheological simplicity and the use of the Kohlraush–Williams–Watts (KWW)[17] relaxation function) but introduces a new hypothesis regarding the state attained at infinite time in the structural relaxation process at a temperature T_a. In the SH model this limit state is identified with the extrapolation to T_a of the equilibrium line experimentally determined at temperatures above T_g. This is simply a result of the identification of the limit of the fictive temperature T_f (see references [6–9]) at infinite time with T_a. In order to introduce a new hypothesis in this regard, the equations of the model in references [10–12] are expressed in terms of the configurational entropy of the system $S_c(t)$ instead of the fictive temperature $T_f(t)$. The model is thus able to introduce different expressions for

* To whom correspondence should be addressed

the value of the configurational entropy attained at infinite time in the structural relaxation process S_c^{lim} (see below).

For a multiple-step thermal history, $T(t) = T_0 + \sum_{i=1}^{n}(T_i - T_{i-1})h(t - t_{i-1})$ (h being the Heaviside unit step function), the configurational entropy $S_c(T)$ turns out to be[10]

$$S_c(t) = S_c^{lim}(T(t)) - \sum_{i=1}^{n} (S_c^{lim}(T_i) - S_c^{lim}(T_{i-1}))\cdot\phi(u(t) - u(t_{i-1})) \quad (1)$$

where $u(t)$ is a reduced time

$$u(t) = \int_0^t \frac{d\sigma}{\tau(\sigma)} \quad (2)$$

where ϕ is a relaxation function of the Kohlrausch–Williams–Watts type[17]

$$\phi(u) = \exp(-u^{\beta}) \quad (3)$$

and $S_c^{lim} = S_c^{lim}(T)$ is the value of the configurational entropy S_c in the state limit of the structural relaxation process for annealing temperature T.

In equation (2), we assume for τ a dependence on the instantaneous values of configurational entropy and temperature given by the equation,

$$\tau(S_c,\ T) = A \exp\left(\frac{B}{S_c T}\right) \quad (4)$$

equation (4) is an extension of Adam and Gibbs' expression[15] for the equilibrium relaxation times to states out of equilibrium.

When the configurational entropy S_c in equation (4) has the equilibrium value $S_c^{eq}(T)$, one has

$$\tau(S_c^{eq}(T),\ T) = \tau^{eq}(T) = A \exp\left(\frac{B}{S_c^{eq}(T) T}\right) \quad (5)$$

and for the configurational entropy in equilibrium states

$$S_c^{eq}(T) = \int_{T_2}^{T} \frac{\Delta c_p(\theta)}{\theta} d\theta \quad (6)$$

is valid. In this equation T_2 is the Gibbs–DiMarzio transition temperature[18], $\Delta c_p(T) = c_{pl}(T) - c_{pg}(T)$ is the configurational heat capacity, and c_{pl} is the heat capacity in the liquid state. $c_{pl}(T)$ is a well-defined and experimentally measurable function for temperatures $T > T_g$.

When in equation (multstep) $S_c^{lim}(T) = S_c^{eq}(T)$, the model equations essentially reduce to those of the SH model[10,19]. Nevertheless it has been shown that in many polymers the fit to the experimental results is highly improved when $S_c^{lim}(T)$ is significantly higher than $S_c^{eq}(T)$[10–12,20], the shape of $S_c^{lim}(T)$ is schematically shown in *Figure 1*. The slope $dS_c^{lim}(T)/dT$ in the glassy state is $(\Delta c_p(T) - \delta)/T$ (while $dS_c^{eq}(T)/dT = \Delta c_p(T)/T$) where δ is a fitting parameter. The details of the calculation procedure and the fitting routine have been explained elsewhere[11,12,20].

EXPERIMENTAL

The epoxy resin was a diglycidyl ether of bisphenol A modified type (CIBA-GEIGY Araldite CY225) with an epoxy equivalent of 188 g/eq and a viscosity at 25°C (Hoepler) of 11540 mPas. A hardener derived from methyltetrahydrophthalic anhydride with an accelerator (CIBA-GEIGY HY225) was used to cure the resin. Both components were commercial products and were used as received without purification.

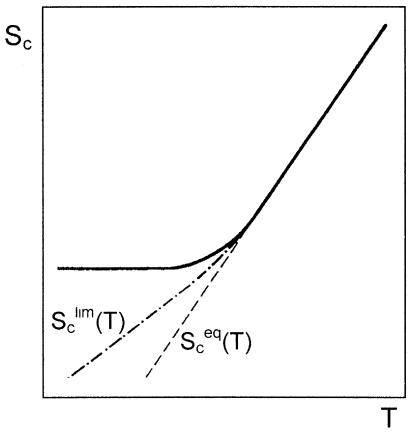

Figure 1 Sketch of the configurational entropy corresponding to the liquid state (dashed line), to an experimental cooling scan at a finite cooling rate (solid line), and to the hypothetical line of the limit states of the structural relaxation process (dashed–dotted line)

Resin and hardener were mixed at a weight ratio of 10 : 8. The mixture was stirred at room temperature for 20 min, and then degassed in a vacuum oven at room temperature for 15 min. The curing of the epoxy resin was carried out in one stage: about 10 mg of sample were enclosed in aluminium DSC pans, introduced in Pyrex tubes under nitrogen atmosphere, and left in a thermostatic bath at 13°C for 8 h. These curing conditions ensure that the resin becomes practically fully cured; this means that no residual exothermic reaction is detected in a DSC scan when the cured sample is heated up to 260°C as shown previously[21,22]

The dynamic-mechanical experiments were performed in a Polymer Laboratories Dynamic Mechanical Thermal Analyzer DMTA-II in the double cantilever mode, with a free length of 5 mm. Measurements were conducted isothermally. The temperature varied from 60 to 130°C in steps of 5°.

A General Radio 1689M was used in the dielectric experiments. The measurements were conducted from 50 to 170°C during a heating scan at 0.1°C/min. Each measurement of the capacity and loss tangent in the whole frequency interval (from 12 to 10^5 Hz) took place in less than 1 min. The curves of permittivity as a function of frequency were thus considered as isotherms.

RESULTS

The experimental DSC thermograms that we analyse in this work were previously reported in references [13,14]. In order to carry out model fitting calculations, seven experimental thermograms were selected, corresponding to thermal histories that include an isothermal annealing at 50°C for 24 480 min (*Figure 2a*), 70°C for 1440 (*Figure 2b*) and 5760 min (*Figure 2c*), 80°C for 600 (*Figure 2d*) and 5760 min (*Figure 2e*) and 90°C for 3660 min (*Figure 2f*). The result of a reference scan was also included (*Figure 2g*). The thermograms are presented in the form of the measured heat flow normalized with the mass of the sample and divided by the heating rate, thus in specific heat units but still arbitrarily shifted in the y-axis.

In this work, a linear dependence of the specific heat capacity on temperature is assumed, both in the glassy and the liquid state and consequently also for the conformational

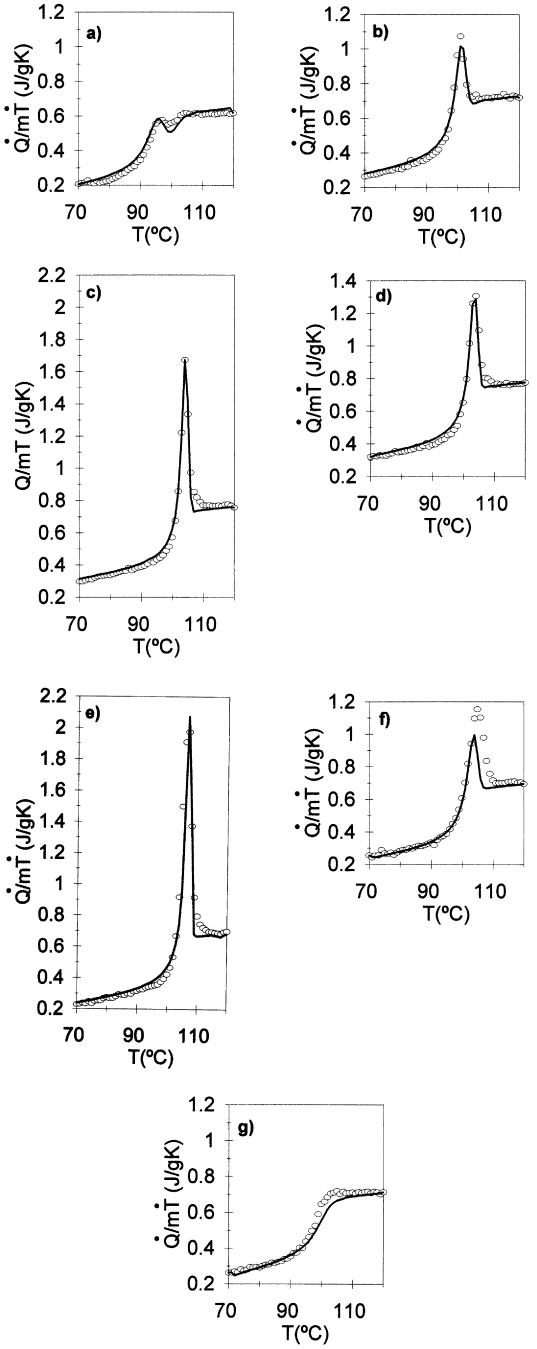

Figure 2 Experimental thermograms measured for the epoxy resin after thermal histories that include an isothermal annealing at: (a) 50°C for 24480 min, (b) 70°C for 1440 and (c) 5760 min, (d) 80°C for 600 and (e) 5760 min, and (f) 90°C for 3660 min. The result of a reference scan was also included (g).The solid line represents the prediction of the model with $B = 2500$ J/g and the remaining parameters are according to *Table 3*

heat capacity, Δc_p. The specific heat capacity in the liquid state was determined in each thermogram by least squares in the temperature interval between 115 and 130°C; the temperature interval between 10 and 70°C was selected for the determination of the heat capacity in the glassy state. The conformational heat capacity was calculated in each thermogram as the difference $\Delta c_p(T) = c_{pl}(T) - c_{pg}(T)$. The average of the lines determined in each of the seven experimental thermograms shown in *Figure 2*, $\Delta c_p(T) = 0.8041 - 0.001342T$ (J/g K) (with T in K) was used in model calculations.

The real and imaginary parts of Young's modulus as a function of frequency are represented in *Figure 3a* and *b*, respectively, in the temperature interval corresponding to the main dynamic-mechanical relaxation (several isotherms are not shown). These curves were used to build master curves by application of the time–temperature superposition principle[23] with the aim of getting a better characterization of the shape of the relaxation curve. The different E'' isotherms were superposed on the 100°C ones by means of horizontal shifts (*Figure 3c*). The values of $\log a_T$ as a function of temperature are shown in *Table 1*. The maximum of E'' at 100°C appears at a frequency of 0.18 Hz (an angular frequency of $\omega_{max} = 1.1\ s^{-1}$). The master curves were fitted to the KWW model

$$\frac{E^*(\omega) - E_g}{E_l - E_g} = \int_0^\infty \dot{\phi}(t) e^{i\omega t} dt,\ \phi(t) = \exp\left(-\left(\frac{t}{\tau}\right)^\beta\right) \quad (7)$$

with E_l and E_g the real part of the Young's modulus in the liquid and the glassy states, respectively. The evaluation of the integral in equation (7) was performed according to

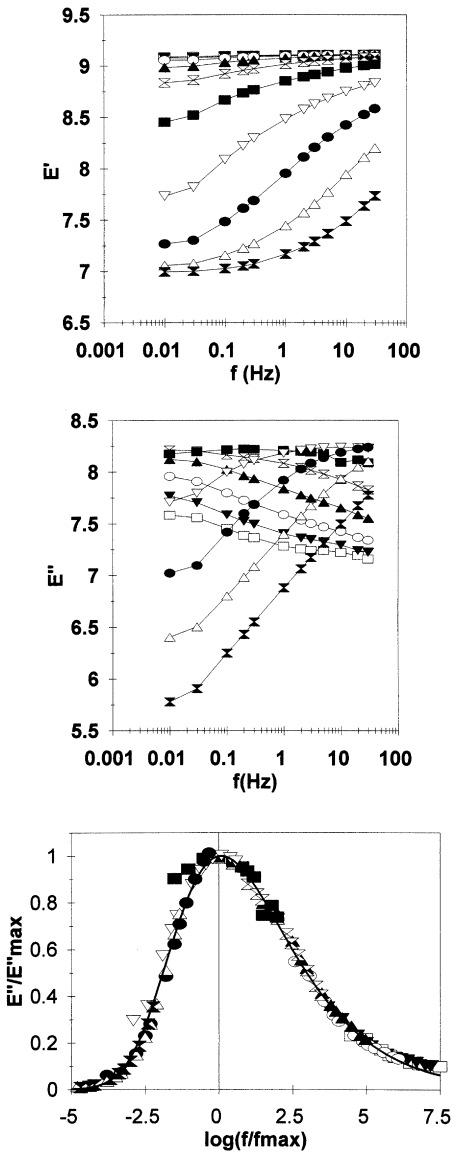

Figure 3 Frequency dependence of the real E' (a) and imaginary E'' (b) parts of the complex Young's modulus measured at 75 (□), 80 (▼), 85 (○), 90 (▲), 95 (⧗), 100 (■), 105 (▽), 110 (●), 115 (△) and 120°C (⧗). The master curve for E'' made by superposition on the 100°C isotherm is shown in (c)

Table 1 Horizontal shift factors, $\log a_T$, needed to superpose each E'' isotherm on the 100°C one to draw the master curve of *Figure 3c*

T (°C)	$\log a_T$
75	6
80	5.2
85	4.1
90	3
95	1.5
100	0
105	− 1.4
110	− 2.3
115	− 3.3
120	− 4.2

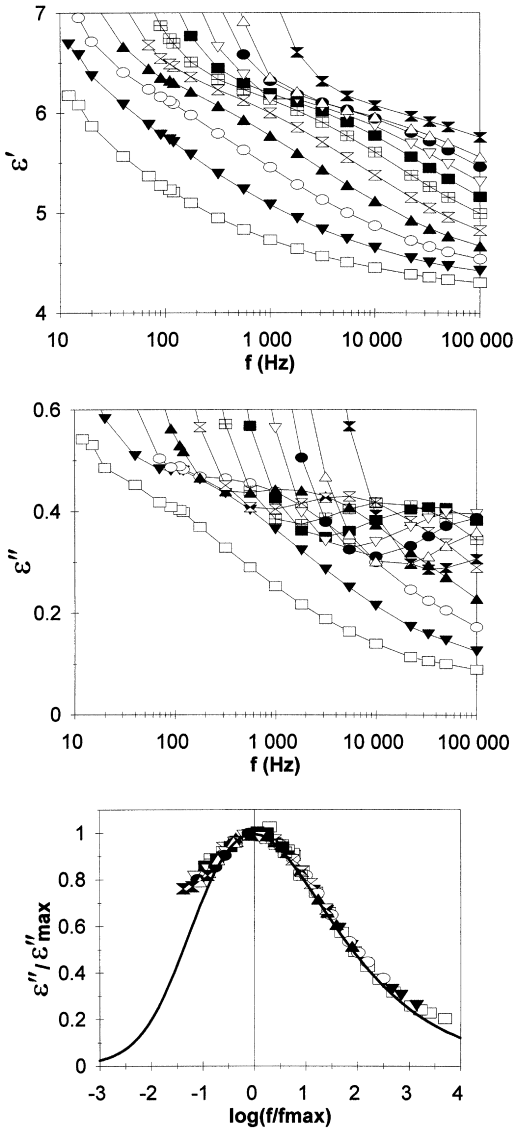

Figure 4 Frequency dependence of the real ε' (a) and imaginary ε'' (b) parts of the complex dielectric permittivity measured at 121.0 (□), 126.0 (▼), 131.0 (○), 135.9 (▲), 140.9 (⧗), 146.0 (⊞), 150.9 (■), 156.0 (▽), 160.9 (●), 166.0 (△) and 175.8°C (⧗). The master curve for ε'' made by superposition on the 146°C isotherm is shown in (c)

reference [24] and the value of the parameter β was determined with a least squares routine. Values of $\beta_M = 0.22$ and $\log(\omega_{max}\tau_M) = -0.27$ were found (we add the subindex M to refer to the dynamic-mechanical relaxation). Thus, the value of τ_M at 100°C was 0.49 s. The values of the parameter τ_M (we will call it relaxation time) for other

Table 2 Horizontal shift factors, $\log a_{T\varepsilon}$ and $\log a_{TDM}$ needed to superpose each ε'' isotherm on the 146°C one to draw the master curve of *Figure 4c*

T (°C)	$\log a_{T\varepsilon}$	$\log a_{TDM}$
121	2.8	2.7
126	2.25	2.1
131	1.6	1.45
136	1	0.9
141	0.5	0.4
146	0	0
151	− 0.35	− 0.4
156	− 0.8	− 0.8
161	− 1	− 1.05
166	− 1.3	− 1.3
176	− 1.8	− 1.8
186	− 2.3	− 2.3

temperatures were calculated from the values of the shift factor $\log a_T$.

The real and imaginary parts of the complex dielectric permittivity as a function of frequency for temperatures ranging between 121.0 and 175.8°C are shown in *Figure 4a* and *b*, respectively. The main relaxation region is followed in its low-frequency side by a sharp increase of both components of the complex permittivity due to free charge motions in the material. The separation of the dipolar and d.c. components of the complex dielectric permittivity requires an empirical equation to be assumed for the d.c. contribution ε''_{dc} to ε''. It was found that the uncertainty in the determination of ε''_{dc} from the ε'' experimental data in the low-frequency region may significantly affect the shape of the low-frequency side of the $\varepsilon'' - \varepsilon''_{dc}$ curve which is assumed to be due to the main relaxation process. Thus, the procedure to discount the d.c. component from the experimental result did not significantly increase the frequency interval in which the main relaxation process can be studied. In order to built a master curve and calculate the β parameter of the KWW equation, only the experimental data around the maximum in the ε'' versus f plot and in the high frequency side were considered, as shown in *Figure 4c*. In this frequency range the values of ε''_{dc} are small as this component is inversely proportional to the frequency.

When the dielectric modulus is calculated from the permittivity data:

$$M^* = \frac{1}{\varepsilon^*},\ M' = \frac{\varepsilon'}{\varepsilon'^2 + \varepsilon''^2},\ M'' = \frac{\varepsilon''}{\varepsilon'^2 + \varepsilon''^2} \qquad (8)$$

the increase in permittivity due to the free charge motion appears in the imaginary part of the dielectric modulus as a narrow peak at frequencies lower than the ones corresponding to the main dielectric relaxation. Only small differences between the dielectric modulus and the dielectric permittivity isotherms in the zone of the main relaxation were found and, thus, no new figures have been included. These differences are reflected in the value of the parameter β of the KWW equation (the value determined from the permittivity data is $\beta_\varepsilon = 0.33$ whereas the value calculated from the dielectric modulus data is $\beta_{DM} = 0.30$). The relaxation times were calculated following the procedure described above. The master curves were built by superposition on the 146°C isotherm and the shift factors are shown in *Table 2*. The value of $\log(\omega_{max}\tau)$ is approximately 0.2 for the values of β found for the dielectric relaxation, which allows the determination of the parameter τ in the dielectric equivalent of equation (7) at 146°C. A value of

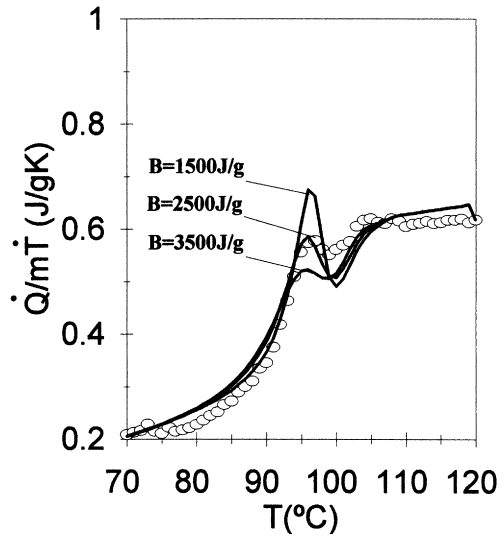

Figure 5 Thermograms predicted by the model for the thermal history with annealing at 50°C for 24480 min. The experimental data are represented as open circles. The model calculations with $B = 1500$, 2500 and 3500 J/g (and the rest of parameters as in *Table 3* for each value of *B*) are represented by solid lines. The height of the peak increases for lower values of the parameter *B*, allowing the identification of the different curves

Table 3 Model parameters found by the search routine for each value of the parameter *B*. The value of the parameter δ (see *Figure 1*) was 0.13 ± 0.01 J/g K for all values of *B*

B (J/g)	β	T_2 (°C)	ln *A* (s)	$T_g - T_2$ (°C)	T_g/T_2
1000	0.38	44.1	− 45.9	53.9	1.17
1500	0.41	29.7	− 52.4	68.3	1.23
2000	0.44	17.6	− 57.3	80.4	1.28
2500	0.47	7.2	− 61.3	90.8	1.32
3000	0.49	− 2.2	− 64.6	102.2	1.37
3500	0.51	− 10.7	− 67.5	108.7	1.41
4000	0.53	− 18.5	− 69.9	116.5	1.46

$\tau_\varepsilon = 8.5 \times 10^{-6}$ s was found from the dielectric permittivity data and $\tau_{DM} = 2 \times 10^{-6}$ s from the dielectric modulus.

DISCUSSION

The set of parameters of the model was determined by a simultaneous least-squares fit to the set of seven experimental $c_p(T)$ curves shown in *Figure 2*. Because of the problem of correlation between parameters, reported also for other polymers[10–12] and similar to that observed for other phenomenological models such as those of Narayanaswamy–Moynihan or Scherer–Hodge[4–7,9,25–29], the parameter *B* was fixed while the other parameters were calculated with the least-squares routine. The fitting procedure was conducted using the Nedler and Mead search routine[30], and the parameter values are given in *Table 3* for the various fixed values of *B* selected.

A typical illustration of the kind of fit obtained is shown as the full lines in *Figure 2*, for the particular case with $B =$ 2500 J/g. The important point here is that the same set of parameter values with the present configurational entropy model gives a reasonably good fit to all seven sets of experimental data at different aging times and temperatures. This should be contrasted with the predictions of the usual model with the assumption of $S_c^{lim}(T) = S_c^{eq}(T)$ which yields rather a poor fit to the experimental DSC curves for any value of the parameter *B*, since it is not possible to reproduce simultaneously the thermograms measured after annealing at different temperatures and for different ageing times.

The model simulated thermograms are drawn to be coincident with the experimental ones at high temperatures, in the liquid state. A small difference in the glassy state between experimental and model simulated curves appears because the conformational specific heat has been calculated as an average of the values determined from all the thermograms.

The value of the parameter δ, 0.13 ± 0.01 J/g K, is nearly independent of the value of *B* fixed in the search routine. This value represents approximately one-third of the total heat capacity increment at the glass transition temperature, a proportion slightly lower than the one found in some thermoplastic polymers[10–12,20].

The values of the set of three parameters β, T_2 and *A* found by the least-squares fitting routine depend systematically on the value of the parameter *B* selected, as can be seen in *Table 3*. Nevertheless, the thermograms predicted by the model with the different sets of parameter values in *Table 3* are nearly coincident for all but one of the thermal treatments considered here, so that for most thermal treatments the model prediction is rather insensitive to the parameter *B*. The exception is the thermogram following the annealing at 50°C (*Figure 2a*), the lowest of the annealing temperatures, which appears particularly sensitive to *B*. This is illustrated in *Figure 5* for some of the values used to compile *Table 3*, where it can be seen that the sub-T_g peak height increases significantly as the value of *B* is reduced. The value of $B = 2500$ J/g in *Figure 2* was selected from a comparison of the experimental data in *Figure 2a* with the theoretical predictions in *Figure 5*.

As a further check on the ability of this model to reproduce the overall structural relaxation behaviour of this epoxy resin, the set of parameters found by the search routine was used to reproduce the complete set of results reported in references [13,14]. The position of the endothermic peak appearing in the DSC thermogram is represented in *Figure 6a–c* as a function of the annealing time for three annealing temperatures, for experimental results and model prediction. The enthalpy increment in the isothermal stage prior to the heating scan is represented in *Figure 7* again for the experimental data and model predictions, with the different symbols representing the different annealing temperatures. The generally good agreement between experimental data and model prediction is noteworthy, taking into account that only a small part of the experimental data was included in the fitting routine.

The dependence on the annealing time of the temperature of the endothermic maxima in the thermograms (*Figure 6a–c*) and of the enthalpy increment in the isothermal stage (*Figure 7*) can be used for an estimation of the Narayanaswamy parameter *x*, using the peak shift method[31,32]. The fact that the experimental results and the model predictions are in close agreement implies that the same value of the parameter *x* can be applied in both cases. The analysis of the experimental data[14] yielded a value of $x = 0.44$ essentially independent of annealing temperature.

The parameters *B*, β, T_2 and ln *A* found from the fitting routine determine the dependence of the equilibrium relaxation time on temperature, shown in *Figure 8* as log τ versus reciprocal temperature for selected values of the parameters in *Table 3*. These curves are remarkably coincident in the whole range of the time interval, indicating

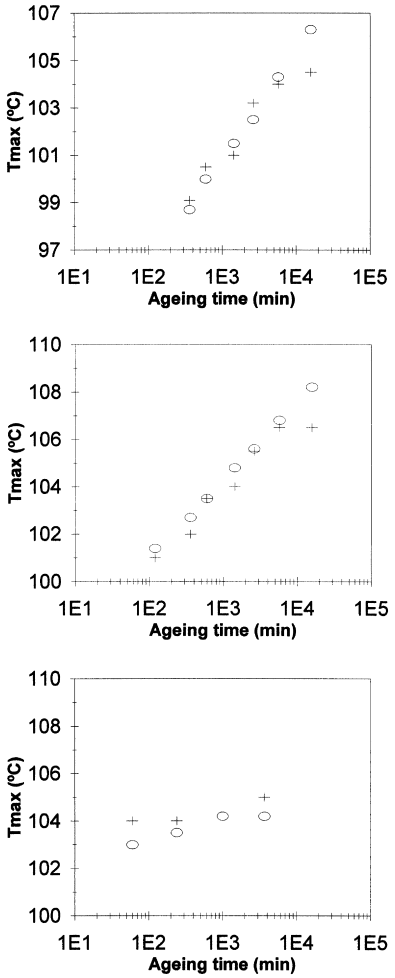

Figure 6 Temperature of the maximum of the thermogram at various annealing temperatures as a function of the annealing time: (a) 70°C, (b) 80°C, (c) 90°C. (+) Experimental data, (○) model simulation

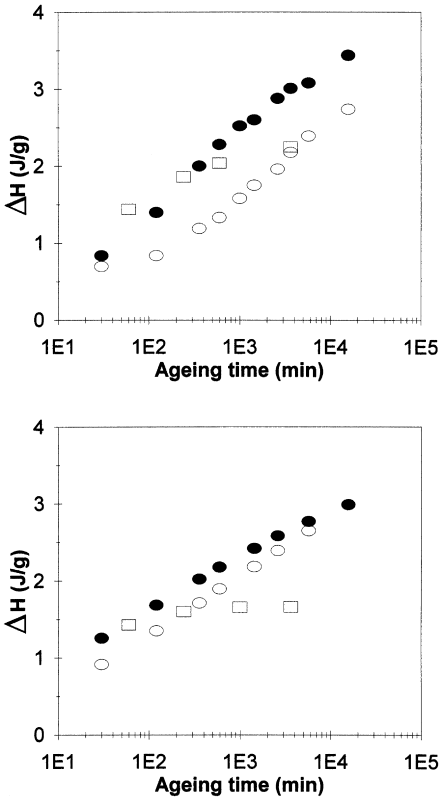

Figure 7 Temperature dependence of the enthalpy increment ΔH during the isothermal stage prior to the measuring scan: (a) experimental data from reference [14], (b) model simulation with $B = 2500$ J/g and the rest of the parameters as shown in *Table 3*. Annealing temperature $T_a = 70$°C (○); 80°C (●); 90°C (□)

that the equilibrium relaxation times are sensitive to the set of parameter values only in a time interval clearly outside the range of experimental times. Within this time interval, therefore, by fitting the model to the experimental data for the epoxy resin we are able to define a single curve of relaxation times, which is compatible with different sets of the three parameters B, T_2 and $\ln A$.

The fitting procedure clearly gives rise to some uncertainty in the values of these parameters. To a certain extent this is improved when lower annealing temperatures are considered (cf. *Figure 2a*, *Figure 5*), which leads to an optimum value of $B = 2500$ J/g. Additional information is also available from other techniques, though. Studies of viscoelastic and dielectric relaxation times suggest that for 'fragile' (in the sense of Angell's classification[33]) materials such as polymer glasses, the ratio T_g/T_2 should range between 1.1 and 1.3. From *Table 3* this would place a higher limit on the parameter B of about 2500 J/g. Although the best fit corresponds to this value of B the sets of parameters found with lower values of this parameter show lower values, and perhaps more reasonable values, for the difference $T_g - T_2$ and for the pre-exponential factor A.

The dynamic-mechanical and dielectric data reported here can also be represented in the form of a temperature dependence of relaxation times, as shown in *Figure 8*. It can be seen that good agreement is obtained between the dynamic-mechanical relaxation times and the calorimetric relaxation times, but that the dielectric relaxation and retardation times are much longer. At temperatures below T_g the dynamic-mechanical experiment is made in a non-equilibrium situation with higher free volume than in equilibrium at the same temperature and consequently the mechanical relaxation time is shorter than it would be in equilibrium. Three points corresponding to the glassy state have been included in *Figure 8*. The values of the relaxation times at these temperatures were calculated from the horizontal shift factor following the same procedure as the rest of the points, as explained above. The consequence of this change of behaviour in the glass transition temperature range is a change in the slope of the $\log \tau$ versus T^{-1} diagram or in the apparent activation energy of the relaxation process as has often been reported with viscoelastic and dielectric techniques[34–36]. An isothermal ageing experiment in which the dynamic-mechanical spectrum is measured after different ageing times would allow the evaluation of the relaxation times with increasing ageing time. Such calculations have been made frequently ever since the work of Struik[37] (see for instance references[38–41]). The change of slope shown in the $\log \tau$ versus T^{-1} diagram by the calorimetric relaxation times evaluated in the limit states of the structural relaxation process (open symbols in *Figure 8*) has a different meaning. In this case this behaviour is parallel to the change of slope in $S_c^{\lim}(T)$ (the dashed–dotted line in *Figure 1a*) as the relaxation times in the limit states are calculated as

$$\tau^{\lim}(T) = A \exp\left(\frac{B}{S_c^{\lim}(T)T}\right) \tag{9}$$

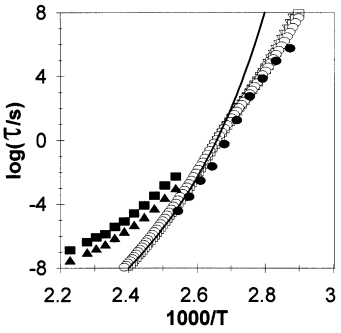

Figure 8 Temperature dependence of the relaxation times in the limit states of the structural relaxation process determined by the model for different values of B (see text): 1500 J/g (▽); 2500 J/g (□); 3500 J/g (○). The equilibrium calorimetric relaxation times calculated with $B = 2500$ J/g are shown by the solid line. The relaxation times of the main dynamic-mechanical (●) and dielectric (■, permittivity), (▲, dielectric modulus) relaxations are also shown

The β parameter in the KWW equation is correlated with the value of B, increasing from 0.38 to 0.53 as B increases from 1000 to 4000 J/g. The calculated values of β agree very well with the value of β estimated between 0.3 and 0.456 from the calorimetric DSC experiments shown in reference[14] and calculated by the method of Hutchinson et al. from intrinsic cycles[42]. These calorimetric values for β are higher than those determined from dielectric or dynamic-mechanical relaxation. Again, as the value of B decreases, the value of β approaches the values found with dielectric and dynamic-mechanical techniques.

CONCLUSIONS

The structural relaxation of a fully cured epoxy resin during isothermal annealing at temperatures within and below the glass transition region has been described using a new model in which the limiting configurational entropy deviates from a linear temperature dependence. On this basis, it is possible to fit reasonably well a wide range of annealing times and temperatures using a single set of parameter values. The equilibrium calorimetric relaxation times derived from this model are in good agreement with those derived from dynamic-mechanical experiments, but dielectric relaxation times are found to be significantly longer.

ACKNOWLEDGEMENTS

This work was supported by CICYT project MAT 94-0596 and DGICYT project no. PB93-1241.

REFERENCES

1. Moynihan, C. T., Macedo, P. B., Montrose, C. J., Gupta, P. K., DeBolt, M. A., Dill, J. F., Dom, B. E., Drake, P. W., Easteal, A. J., Elterman, P. B., Moeller, R. P. and Sasabe, H., *Ann. N.Y. Acad. Sci.*, 1976, **279**, 15.
2. Kovacs, A. J., Aklonis, J. J., Hutchinson, J. M. and Ramos, A. R., *J. Polym. Sci., Polym. Phys.*, 1979, **17**, 1097.
3. Scherer, G. W. J., *Am. Ceram. Soc.*, 1984, **67**, 504.
4. Hodge, I. M., *Macromolecules*, 1987, **20**, 2897.
5. Hodge, I. M., *J. Non-Cryst. Solids*, 1994, **169**, 211.
6. Prest, W. M., Roberts, Jr., F. J. and Hodge, I. M., in *Proceedings of the 12th NATAS Conference*, Williamsburg, VA, 1980, pp. 119–123.
7. Tribone, J. J., O'Reilly, J. M. and Greener, J., *Macromolecules*, 1986, **19**, 1732.
8. Romero Colomer, F. and Gómez Ribelles, J. L., *Polymer*, 1989, **30**, 849.
9. Gómez Ribelles, J. L., Ribes Greus, A. and Díaz Calleja, R., *Polymer*, 1990, **31**, 223.
10. Gómez Ribelles, J. L. and Monleón Pradas, M., *Macromolecules*, 1995, **28**, 5867.
11. Gómez Ribelles, J. L., Monleón Pradas, M., Más Estellés, J., Vidaurre Garayo, A., Romero Colomer, F. and Meseguer Dueñas, J. M., *Polymer*, 1997, **38**, 963.
12. Meseguer Dueñas, J. M., Vidaurre Garayo, A., Romero Colomer, F., Más Estellés, J., Gómez Ribelles, J. L. and Monleón Pradas, M., *J. Polym. Sci. Polym. Phys. Ed.*, 1997, **35**, 2201.
13. Montserrat, S., *Progr. Colloid Polym. Sci*, 1992, **87**, 78.
14. Montserrat, S., *J. Polym. Sci. Polym. Phys. Ed.*, 1994, **32**, 509.
15. Adam, G. and Gibbs, J. H., *J. Chem. Phys.*, 1965, **43**, 139.
16. Narayanaswamy, O. S., *J. Am. Ceram. Soc.*, 1971, **54**, 491.
17. Williams, G. and Watts, D. C., *Trans. Faraday Soc.*, 1970, **66**, 80.
18. Gibbs, J. H. and DiMarzio, E. A., *J. Chem. Phys.*, 1958, **28**, 373.
19. Gómez Ribelles, J. L., Monleón Pradas, M., Más Estellés, J., Vidaurre Garayo, A., Romero Colomer, F. and Meseguer Dueñas, J. M., *Macromolecules*, 1995, **28**, 5878.
20. Brunacci, A., Cowie, J. M. G., Ferguson, R., Gómez Ribelles, J. L. and Vidaurre, A., *Macromolecules*, 1996, **29**, 7976.
21. Montserrat, S., *J. Therm. Anal.*, 1991, **37**, 1751.
22. Montserrat, S., *J. Appl. Polym. Sci.*, 1992, **44**, 545.
23. Ferry, J. D., *Viscoelastic Properties of Polymers*. Wiley, New York, 1970.
24. Williams, G., Watts, D. C., Dev, S. B. and North, A. M., *Trans. Faraday Soc.*, 1971, **67**, 1323.
25. Moynihan, C. T., Crichton, S. N. and Opalka, S. M., *J. Non-Cryst. Solids*, 1991, **420**, 131–133.
26. Hodge, I. M. and Berens, A. R., *Macromolecules*, 1982, **15**, 762.
27. Hodge, I. M. and Huvard, G. S., *Macromolecules*, 1983, **16**, 371.
28. Hodge, I. M., *J. Non-Cryst. Solids*, 1991, **435**, 131–133.
29. Más Estellés, J., Gómez Ribelles, J. L. and Monleón Pradas, M., *Rev. Port. Hemorreol.*, 1990, **4**(Suppl. 1/Pt A), 13.
30. Nedler, J. A. and Mead, R., *Comput. J.*, 1965, **7**, 308.
31. Montserrat, S., Cortés, P., Pappin, A. J., Quah, K. H. and Hutchinson, J. M., *J. Non-Cryst. Solids*, 1994, **1017**, 172–174.
32. Hutchinson, J. M. and Ruddy, M., *J. Polym. Sci. Polym. Phys. Ed.*, 1988, **26**, 2341.
33. Angell, C. A., *J. Non-Cryst. Solids*, 1991, **3**, 131–133.
34. Saito, S., *J. Appl. Polym. Sci.*, 1959, **2**, 93.
35. Saito, N., Okano, K., Iwayanagi, S. and Hideshima, T., in *Molecular Motions in Solid State Polymers. Solid State Physics*, Vol. 14, ed. F. Seitz and D. Turnbull. Academic Press, New York, 1963.
36. Schlosser, E., *Polymer Bulletin*, 1982, **8**, 461.
37. Struik, L. C. E., *Physical Ageing in Amorphous Polymers and Other Materials*. Elsevier, Amsterdam, 1978.
38. Gómez Ribelles, J. L. and Díaz Calleja, R., *Polymer Bulletin*, 1985, **14**, 45.
39. Díaz Calleja, R. and Gómez Ribelles, J. L., in *Developments in Plastics Technology—4*, ed. A Whelan and J. P. Goff. Elsevier-Applied Science, London, 1989.
40. McKenna, G. B., *J. Res. Natl. Inst. Stand. Technol.*, 1994, **99**, 169.
41. Hutchinson, J. M., *Prog. Polym. Sci.*, 1995, **20**, 703.
42. Hutchinson, J. M. and Ruddy, M., *J. Polym. Sci. Polym. Phys. Ed.*, 1990, **28**, 2127.